

Transverse-Mode Dynamics in Directly Modulated Vertical-Cavity Surface-Emitting Lasers With Optical Feedback

Maria Susana Torre, Cristina Masoller, Paul Mandel, *Member, IEEE*, and K. Alan Shore, *Senior Member, IEEE*

Abstract—Vertical-cavity surface-emitting lasers (VCSELs) with optical feedback are known to exhibit different transverse-mode regimes depending on the injection current. Close to threshold a VCSEL operates on the fundamental transverse mode, while for larger injection the dynamics is often multimode, with the optical feedback inducing either in-phase or anti-phase transverse mode oscillations. In this paper, we study numerically the influence of current modulation on these different feedback-induced transverse-mode regimes. The modulation amplitude and period are taken as control parameters. We find that the in-phase and anti-phase regimes are robust under weak modulation. As the modulation amplitude increases, there is a transition to a dynamics governed by the current modulation, where the total output power follows the injection current and there is either single-mode or in-phase multimode behavior. However, the effect of the current modulation depends on the modulation period. Under fast modulation, the laser cannot follow the modulation and the optical-feedback-induced effects are dominant. On the contrary, under slow modulation there is a superposition of modulation and feedback effects, with the total output following the modulated current and an underlying transverse-mode behavior mainly determined by the optical feedback. A resonant behavior was observed for modulation periods close to the internal oscillation period. In this case, current modulation induces pulsing output intensity with single-mode or in-phase multimode behavior.

Index Terms—Anti-phase dynamics, dynamical laser instabilities, laser diodes, modulation response, optical chaos, semiconductor lasers, vertical-cavity surface-emitting lasers (VCSELs).

I. INTRODUCTION

THE increasing demand for high data-rate fiber-optic communication systems has motivated the development of a new generation of low-cost, high-performance semiconductor lasers. Vertical-cavity surface-emitting lasers (VCSELs) are attractive sources for high-bit-rate optical data transmission. The

Manuscript received November 19, 2003; revised February 17, 2004. The work of M. S. Torre was supported in part by a grant from Secretaría de Ciencia y Técnica, (UNCPBA-Argentina) and by FONCyT through Grant 3/9598. The work of C. Masoller was supported in part by the EPSRC under Grant GR/S62239/01. The work of P. Mandel was supported by the Fonds National de la Recherche Scientifique and the Interuniversity Attraction Pole Program of the Belgian government.

M. S. Torre is with the Instituto de Física “Arroyo Seco,” U.N.C.P.B.A., Pinto 399 (7000) Tandil, Argentina.

C. Masoller is with the Instituto de Física, Facultad de Ciencias, Universidad de la República, Montevideo 11400, Uruguay, and also with the University of Wales, School of Informatics, Bangor LL57 1UT, U.K.

P. Mandel is with the Université Libre de Bruxelles, Optique Nonlinéaire Théorique, B-1050 Bruxelles, Belgium.

K. A. Shore is with the University of Wales, School of Informatics, Bangor LL57 1UT, U.K.

Digital Object Identifier 10.1109/JQE.2004.828229

advantages of VCSELs over conventional, edge-emitting semiconductor lasers are single-longitudinal-mode operation, low threshold, high modulation efficiency, dense packing capability, and narrow circular beam profile [1].

Near-threshold VCSELs typically emit linearly polarized light in the fundamental transverse mode. However, in many devices, it is observed that the polarization state selected at threshold becomes unstable as the injection current is increased, and a switch to the orthogonal polarization state occurs. The polarization bistability, switching, and competition has been studied by many authors (see, e.g., [2] and references therein). For high-power operation, high-order transverse modes are excited and the VCSEL usually emits multiple transverse modes. An important consideration for the application of multimode VCSELs in high-speed multimode fiber links using multiplexed modulation schemes is the understanding of the effects of external optical feedback on the dynamics of current-modulated multimode VCSELs.

The nonlinear dynamics of edge-emitting semiconductor lasers subjected to both optical feedback and current modulation has been studied by several authors [3]–[11]. While recent attention has been paid to the dynamics of external-cavity VCSELs [12]–[15] and the dynamics of current-modulated VCSELs [16], [17], to the best of our knowledge the combined effects of optical feedback and current modulation have not been studied in VCSELs. The aim of this paper is to study these effects with particular emphasis on multi-transverse-mode operation. As a first step to understand the behavior of current-modulated external-cavity VCSELs, we do not take into account the polarization dynamics, which we plan to include as a second step in future work. Our model is therefore valid for studying transverse effects such as instabilities induced by spatial inhomogeneities, but not for polarization-induced instabilities.

It was recently shown numerically that weak optical feedback from a distant reflector induces distinct transverse-mode dynamical regimes [18]. Close to threshold the VCSEL dynamics is single-mode and optical feedback induces periodic oscillations of the laser output. For larger injection current, the VCSELs dynamics is multimode, and optical feedback induces either in-phase (for low current) or anti-phase (for larger current) transverse mode oscillations. In this paper, we study numerically the effect of current modulation in these dynamical regimes. Our simulations are based on the model of [18], which is an extension of the model originally proposed by Valle *et al.* [19], [20]. The model includes spatial profiles for both the

transverse modes and the carrier density. The model applies to index-guided VCSELS, where the modal spatial profiles and frequencies are determined by the built-in refractive index distribution. The model includes external optical feedback as in the Lang–Kobayashi approach [21], taking into account a single reflection in the external cavity.

The modulation amplitude and the modulation period were taken as control parameters. Our results show that weak modulation preserves the feedback-induced regimes (periodic single-mode oscillations, as well as in-phase and anti-phase multimode oscillations), but as the modulation amplitude increases there is a transition to a dynamics that is governed by the current modulation. For sufficiently strong modulation, the laser output follows the injection current and the dynamics is either single-mode or multi-mode. In the latter case, transverse-mode oscillations are in phase. However, the effect of the modulation depends on the modulation period: when the modulation period is close to the period of the feedback-induced oscillations, a resonant pulsing behavior is observed. This resonance was recently studied numerically in the framework of a simplified rate equation model for a single-mode laser with optical feedback and optical injection [22].

This paper is organized as follows. The model used in this study is described in Section II. Section III presents the results of the numerical simulations on the effects of current modulation on the single-mode, in-phase, and anti-phase optical feedback-induced regimes. Section IV contains a summary and the conclusion.

II. MODEL

We consider a cylindrically symmetric structure, whose active region [consisting of several quantum wells (QWs)] is modeled as a single effective QW of radius a and thickness d_{qw} . Barrier regions of thickness d_b limit the QW region. Two highly reflecting mirrors separated by a distance L along the longitudinal z axis define the laser cavity. The injected current is

$$j(r, t) = j_o \left[1 + \delta \sin \left(\frac{2\pi t}{T_{\text{mod}}} \right) \right], \quad \text{for } r < a$$

$$j(r, t) = 0, \quad \text{otherwise} \quad (1)$$

where δ is the amplitude of the modulation ($0 < \delta < 1$) and T_{mod} is the period of the modulation.

The emission behavior is determined by the built-in index guiding introduced by transverse refractive index step in the surrounding region. The core (cladding) refractive index is taken to be $n_{\text{core}}(n_{\text{clad}})$, i.e., the transverse refractive index profile is $n(r) = n_{\text{core}}$ for $r < a$ and $n(r) = n_{\text{clad}}$ for $r > a$. For this geometry, the appropriate transverse modes are the linearly polarized LP_{mn} modes [23]. To simplify the calculations, we consider that only three modes, having azimuthal symmetry, are excited in the range of parameters considered in this paper as follows:

$$\psi_1(r) \equiv \psi_{01}(r, \theta)$$

$$\psi_2(r) \equiv \psi_{02}(r, \theta)$$

$$\psi_3(r) \equiv \psi_{03}(r, \theta). \quad (2)$$

The mode profiles are normalized such that $\int_0^\infty |\psi_i(r)|^2 r dr = 1$. Since the mode profiles are exponentially small outside the active region, this normalization hardly differs from the physical normalization $\int_0^a |\psi_i(r)|^2 r dr = 1$.

The equations for the slowly varying complex amplitude of the i th mode, $e_i(t)$, the density of carriers confined in the QW region, $n_w(r, t)$, and the density of (unconfined) carriers in the barrier region, $n_b(r, t)$ are [18]

$$\frac{de_i}{dt} = \frac{1 + j\alpha}{2} \left(g_i - \frac{1}{\tau_{pi}} \right) e_i(t) + k_i e_i(t - \tau) \exp(-j\omega_i \tau) \quad (3)$$

$$\frac{\partial n_b}{\partial t} = \frac{j(r, t)}{ed_b} - \frac{n_b}{\tau_{\text{cap}}} + \frac{V_{\text{qw}} n_w}{V_b \tau_{\text{esc}}} - \frac{n_b}{\tau_n} + D_b \frac{1}{r} \frac{\partial}{\partial r} \left(r \frac{\partial n_b}{\partial r} \right) \quad (4)$$

$$\frac{\partial n_w}{\partial t} = \frac{V_b n_b}{V_{\text{qw}} \tau_{\text{cap}}} - \frac{n_w}{\tau_{\text{esc}}} - \frac{n_w}{\tau_n} - g_o(n_w - n_t) \times \sum |e_i|^2 |\psi_i|^2 + D_w \frac{1}{r} \frac{\partial}{\partial r} \left(r \frac{\partial n_w}{\partial r} \right). \quad (5)$$

The first term on the right-hand side of (3) accounts for optical gain, losses, and phase-amplitude coupling. Here, α is the linewidth enhancement factor and g_i is the modal gain, given as follows:

$$g_i(t) = \int_0^\infty g_o \Gamma_i (n_w - n_t) |\psi_i|^2 r dr \quad (6)$$

where g_o is the linear gain coefficient, Γ_i is the confinement factor for the i th mode, and n_t is the transparency carrier density. τ_{pi} is the photon lifetime for the i th mode.

The second term on the right-hand side of (3) takes into account the field reflected from the external cavity. We consider a single reflection and therefore the model is valid for weak to moderate feedback levels, k_i is the feedback coefficient of the i th mode, ω_i is the optical frequency of the i th mode in the absence of feedback, and τ is the external-cavity round-trip time.

The terms on the right-hand side of (4) correspond, from left to right, to: 1) the rate at which carriers are injected into the barrier region; 2) the rate at which carriers are captured into the QWs; 3) the rate at which carriers escape out of the QWs; 4) the carrier loss owing to various nonradiative recombination processes; and 5) the last term accounts for carrier diffusion across the barrier region. The transport effects are included by a capture time τ_{cap} , an escape time τ_{esc} , and a diffusion coefficient D_b . The carrier loss is included by a carrier lifetime τ_n . Since the variables n_b and n_w refer to carrier densities, the different sizes of the barrier and QW regions must be taken into account. This is done by the ratio V_b/V_{qw} , where $V_b = d_b \pi a^2$ is the volume of the barrier region and $V_{\text{qw}} = d_{\text{qw}} \pi a^2$ is the volume of the QW region.

The terms on the right-hand side of (5) correspond, from left to right, to: 1) the carriers captured into the QWs; 2) the carriers that escape out of the QWs; 3) the nonradiative carrier loss; 4) the carrier loss owing to stimulated recombination; and 5) the final term to carrier diffusion across the QWs.

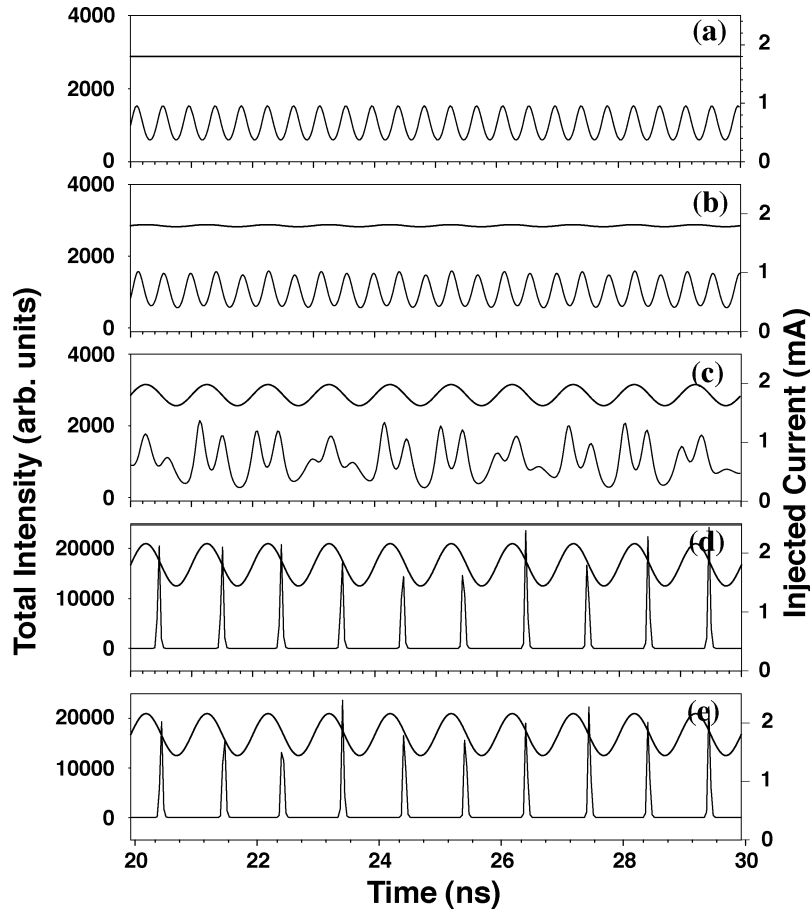


Fig. 1. Laser output power as a function of time for different values of the modulation amplitude. The dc injection current is such that the laser operates on the fundamental transverse mode ($I_0 = 1.8$ mA). The modulation period is $T_{\text{mod}} = 1$ ns. (a) $\delta = 0.0$. (b) $\delta = 0.01$. (c) $\delta = 0.1$. (d) $\delta = 0.2$. (e) $\delta = 0.2$ and no optical feedback ($k = 0$). The thin (thick) line shows the value of the intensity (injection current).

III. NUMERICAL RESULTS

We numerically solve the model equations with typical VCSEL parameters [18]: $a = 6 \mu\text{m}$, $d_{\text{qw}} = 0.024 \mu\text{m}$ (three quantum wells of thickness $0.08 \mu\text{m}$ each), $d_b = 1.2 \mu\text{m}$, index step = 0.1, $\alpha = 3$, $g_o = v_g \partial g / \partial n$ with $v_g = 0.0715 \mu\text{m}/\text{ns}$ and $\partial g / \partial n = 5.95 \times 10^{-8} \mu\text{m}^2$, $n_t = 1.33 \times 10^6 \mu\text{m}^{-3}$, $\tau_{\text{cap}} = 5$ ps, $\tau_{\text{esc}} = 25.5$ ps, $\tau_n = 1.52$ ns, and $D_w = D_b = 0.5 \mu\text{m}^2/\text{ns}$. All modes have the same confinement factor $\Gamma_i = 0.038$ and losses $\tau_{pi} = 2.2$ ps. For these parameters, the threshold current is $I_{\text{th}} = j_{\text{th}} \pi a^2 \sim 1.5$ mA. If not otherwise stated, the external cavity parameters are the same as in [18], which correspond to weak optical feedback: $k_i = k = 1 \text{ ns}^{-1}$, $\tau = 1$ ns, $\omega_i \tau = 0$ rad.

The equations were integrated with a time integration step $\Delta t = 10^{-4}$ ps and a space integration step $\Delta r = 0.02 \mu\text{m}$. Due to carrier diffusion, we needed to integrate (4) and (5) over a space interval $0 < r < na$ with n large enough to assure that $n_w(r = na) \sim 0$ and $n_b(r = na) \sim 0$. The initial conditions are all taken through the paper with the modal fields off (i.e., $e_i(t) = \xi(t)$ for $-\tau < t < 0$, where ξ is a small complex noise source), and the carrier densities are at the transparency value.

We analyzed the effect of current modulation on three different feedback-induced transverse-mode regimes, which occur for increasing values of the dc injection current, $I_0 = j_0 \pi a^2$:

(a) single-mode operation, with periodic oscillations of the fundamental LP_{01} mode; (b) two-mode operation, with in-phase oscillations of the LP_{01} and LP_{02} modes; and (c) three-mode operation, with anti-phase oscillations of the LP_{01} and LP_{02} modes. The modulation amplitude and period are taken as control parameters.

First we consider a dc injection current such that the laser operates in the fundamental LP_{01} mode ($I_0 = 1.8$ mA). Fig. 1(a) displays the laser output as a function of time in the absence of current modulation ($\delta = 0$) and shows that weak optical feedback induces periodic oscillations of the laser output power. The period of the oscillations is close to the period of the relaxation oscillations of the solitary laser ($T_{\text{RO}} \sim 0.43$ ns for $I_0 = 1.8$ mA). Let us now include current modulation: first we fix the modulation period ($T_{\text{mod}} = 1$ ns) and vary the modulation amplitude. As δ increases, Fig. 1(b)–(d) displays a transition from a dynamics that is induced by the optical feedback to a dynamics that is induced by the current modulation. It can be observed that weak modulation [$\delta = 0.01$, Fig. 1(b)] modifies only slightly the periodic oscillations. For larger modulation, there is competition between the effects of optical feedback and current modulation [$\delta = 0.1$, Fig. 1(c)]. Under strong modulation [$\delta = 0.2$, Fig. 1(d)], the laser exhibits a periodic pulsing behavior, with period $\sim T_{\text{mod}}$. The dynamics is governed by the modulation and the laser output is the same as that in the absence of optical

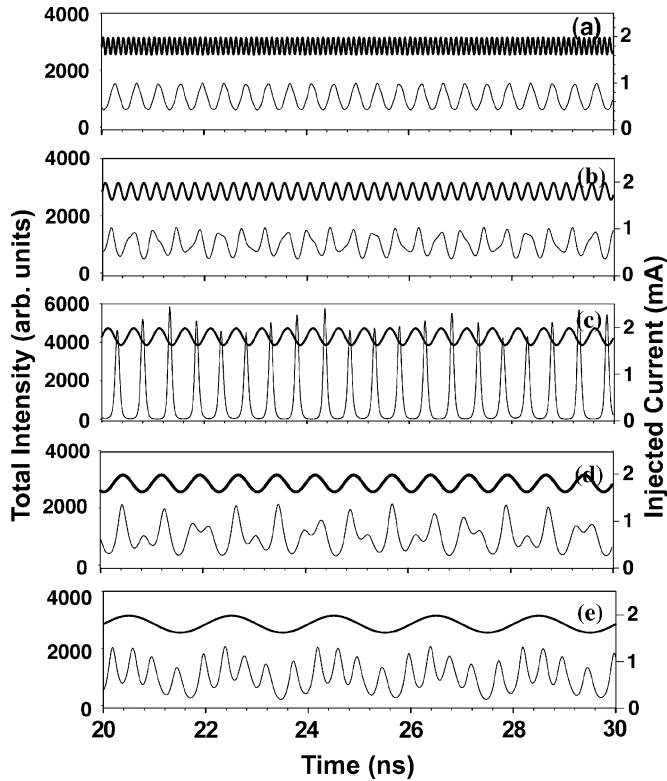


Fig. 2. Laser output power as a function of time for different values of the modulation period. $I_0 = 1.8$ mA and $\delta = 0.1$. (a) $T_{\text{mod}} = 0.1$ ns. (b) $T_{\text{mod}} = 0.25$ ns. (c) $T_{\text{mod}} = 0.5$ ns. (d) $T_{\text{mod}} = 0.75$ ns. (e) $T_{\text{mod}} = 2$ ns. The thin (thick) line shows the value of the intensity (injection current).

feedback [shown for comparison in Fig. 1(e), where $\delta = 0.2$ and $k = 0$].

Next we fix the modulation amplitude and vary the modulation period. Fig. 2 displays the laser output as a function of time for $\delta = 0.1$ and different T_{mod} . For very fast modulation [Fig. 2(a)], the laser cannot follow the modulation and its output is the same as that in the absence of modulation. As the modulation becomes slower, the effect of the modulation becomes increasingly relevant [Fig. 2(b)–(e)]. For sufficiently slow modulation, the dynamics is quasi-periodic: the current modulation induces a slow envelope in the feedback-induced fast oscillations [Fig. 2(e)]. It can be observed that the envelope is in-phase with the injection current. In this case, there is a superposition of optical feedback and current modulation effects, with one frequency predominantly determined by the modulation and the other frequency predominantly determined by the feedback.

It can be observed in Fig. 2(c) that the laser output exhibits large pulses of period T_{mod} , which suggests a resonant behavior. We note also that this occurs for $T_{\text{mod}} = 0.5$ ns, which is close to the period of the relaxation oscillations ($T_{RO} \sim 0.43$ ns). To explore in more detail this behavior, we display in Fig. 3 the average ($\langle I \rangle$), the maximum (I_{max}), and the minimum (I_{min}) values of the intensity oscillations as a function of the modulation period T_{mod} for various values of the modulation amplitude δ and the feedback level k . To clearly distinguish the regions where the oscillations are periodic from regions where the oscillations are more complex, we plot all maxima and minima. When the dynamics is not periodic, there are several (local)

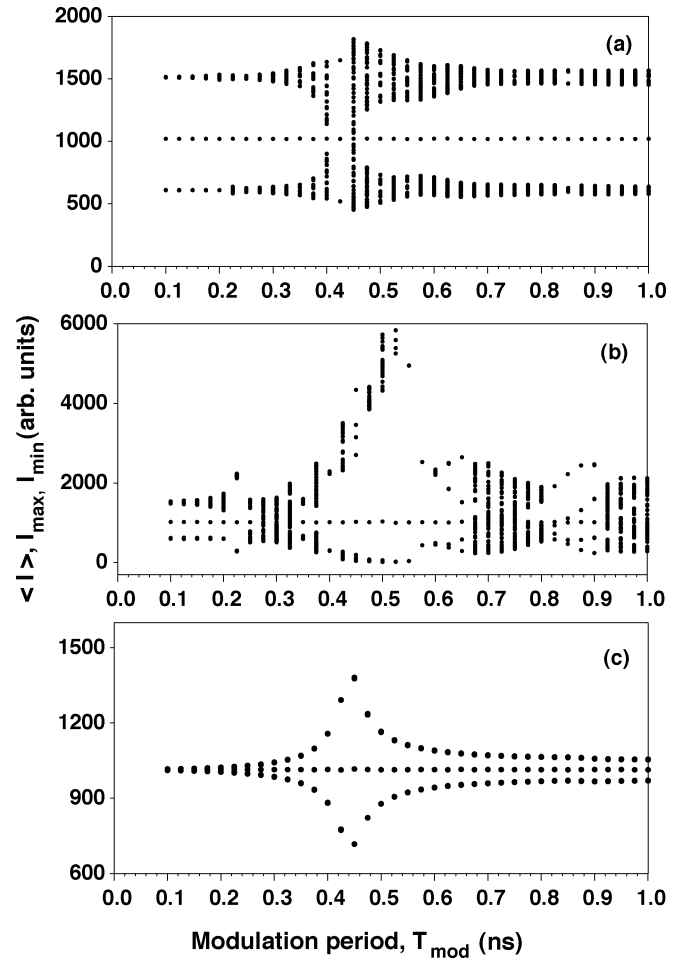


Fig. 3. Maximum, minimum, and average values of the intensity oscillations as a function of the modulation period. $I_0 = 1.8$ mA. (a) $\delta = 0.01$, $k = 1$ ns $^{-1}$. (b) $\delta = 0.1$, $k = 1$ ns $^{-1}$. (c) $\delta = 0.01$, $k = 0.2$ ns $^{-1}$.

maxima and minima. On the contrary, when the dynamics is periodic, there is a single (global) maximum and minimum.

We found that $\langle I \rangle$ is independent of T_{mod} while I_{max} and I_{min} show a complicated dependence on T_{mod} . Fig. 3(a) displays results for weak modulation ($\delta = 0.01$) and the same feedback level as in Figs. 1 and 2 ($k = 1$ ns $^{-1}$). A resonance peak can be observed at $T_{\text{mod}} \sim T_{RO} \sim 0.43$ ns, such that the maximum value of I_{max} coincides with the minimum value of I_{min} . The resonance peak becomes asymmetric for larger modulation amplitude [see Fig. 3(b) which is for $\delta = 0.1$ and $k = 1$ ns $^{-1}$]. The complicated structure of the resonance is due to the optical feedback. Fig. 3(c), which is obtained for the same modulation amplitude as Fig. 3(a) but with a lower feedback level ($\delta = 0.01$, $k = 0.2$ ns $^{-1}$), reveals a simple and symmetric peak, which is what one expects, based on the behavior of a nonlinear oscillator under weak periodic forcing. The resonant behavior for particular values of the modulation period was recently studied in detail in [22], based on a simplified model for a single-mode laser.

It is interesting to study the nature of the transition from “feedback-dominant” to “modulation-dominant” dynamics in the resonant situation $T_{\text{mod}} = T_{RO}$. Fig. 4 displays the laser output for fixed $T_{\text{mod}} = 0.43$ ns and increasing δ . It can be observed that the optical feedback and the current modulation do

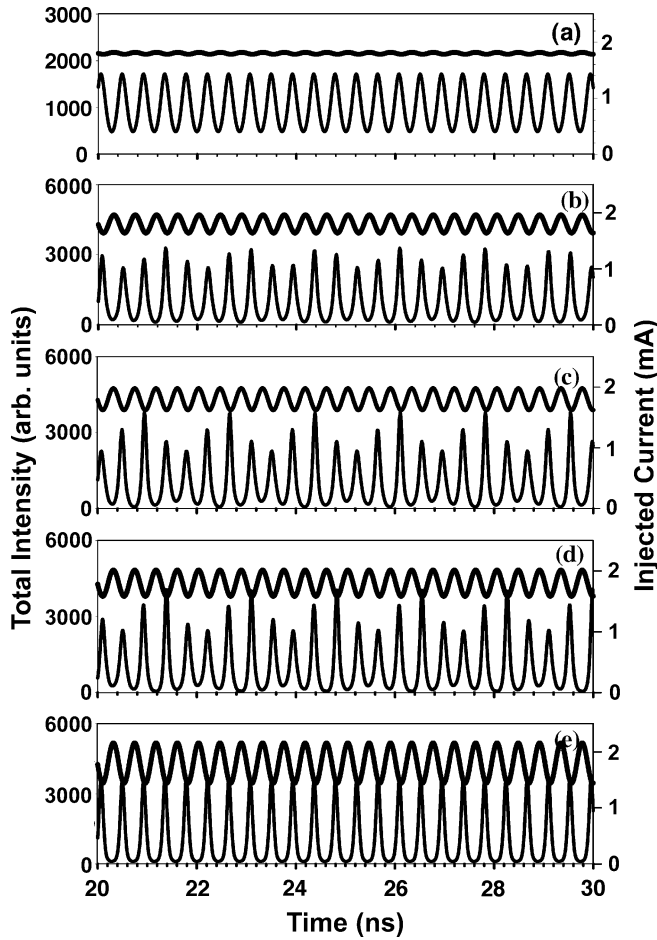


Fig. 4. Laser output power as a function of time for different values of the modulation amplitude. $I_0 = 1.8$ mA and $T_{\text{mod}} = T_{\text{RO}} = 0.43$ ns. (a) $\delta = 0.01$. (b) $\delta = 0.05$. (c) $\delta = 0.1$. (d) $\delta = 0.15$. (e) $\delta = 0.2$. The thick (thin) line shows the value of the intensity (injection current).

not compete but cooperate to induce periodic pulses (of period $T_{\text{mod}} = T_{\text{RO}}$). It can also be observed that the injection current and the laser output power are in exact anti-phase.

Next we consider a larger dc injection current, such that the laser supports two transverse modes (the LP_{01} and LP_{02} modes). Fig. 5(a) shows the dynamics in the absence of current modulation. It can be observed that weak optical feedback induces in-phase oscillations of the modal intensities (the total output power exhibits periodic oscillations of period ~ 0.4 ns). Let us first increase δ while keeping T_{mod} fixed. Fig. 5(b)–(d) illustrates a transition from feedback-induced dynamics to modulation-induced dynamics. Fig. 5(e) displays the dynamics of the solitary laser ($k = 0$) under strong modulation. By comparing Fig. 5(d) and (e), it can be observed that the effect of weak optical feedback is still relevant under strong modulation: without feedback the laser output is quasi-periodic [Fig. 5(e)], while in the presence of optical feedback the laser output exhibits more irregular oscillations. Let us now fix δ and vary T_{mod} . Fig. 6 shows that varying T_{mod} has the same effect as in the single-mode regime: 1) fast modulation does not affect the laser output, which is nearly the same as that of the laser without modulation [Fig. 6(a)]; 2) resonant pulses of period T_{mod} are observed for $T_{\text{mod}} = T_{\text{RO}} \sim 0.4$ ns [Fig. 6(c)]; and 3) a quasi-periodic output occurs for large enough T_{mod} [Fig. 6(e)], with one

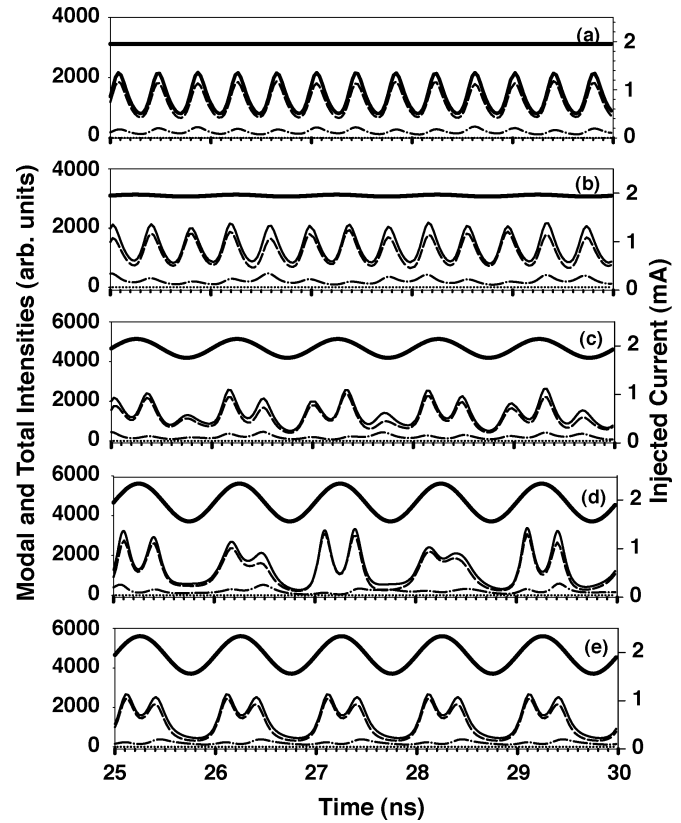


Fig. 5. Total intensity (thin solid line) and modal intensities (LP_{01} : dashed line; LP_{02} : dot-dashed line) as a function of time for different modulation amplitudes. $I_0 = 1.95$ mA and $T_{\text{mod}} = 1$ ns. (a) $\delta = 0.0$. (b) $\delta = 0.01$. (c) $\delta = 0.1$. (d) $\delta = 0.2$. (e) $\delta = 0.2$ and no optical feedback ($k = 0$). The thick line shows the injection current.

frequency determined by the optical feedback and the other frequency determined by the current modulation.

Next, we consider an even larger dc injection current such that the laser supports three transverse modes (the LP_{01} , LP_{02} , and LP_{03} modes). Fig. 7(a) shows that weak optical feedback induces anti-phased oscillations of the LP_{01} and LP_{02} transverse modes. Fig. 7(b)–(d) show the effect of increasing δ for fixed T_{mod} . The anti-phase dynamics is robust under the modulation [Fig. 7(b)–(d)]. Notice that in Fig. 7(c) and (d) the total output power and the injection current are in phase, while there is an underlying anti-phase dynamics of the LP_{01} and LP_{02} modes. It can be observed that the effect of the feedback is still important under strong modulation: without optical feedback, there is an almost in-phase dynamics of the three transverse modes [see Fig. 7(e)].

Fig. 8 shows the effect of varying the modulation period for fixed modulation amplitude. As expected, given the complexity of the multitransverse-mode dynamics, several interesting features can be observed. Fast modulation [Fig. 8(a)] preserves the anti-phase dynamics (but induces small amplitude oscillations at the driving frequency in the modal intensities). For $T_{\text{mod}} = 0.25$ ns, the total intensity exhibits large pulses of period T_{mod} while there are in-phase pulses of the three transverse modes [Fig. 8(b)]. As the modulation becomes slower, the total intensity follows the injection current while there are two different underlying modal behaviors. In Fig. 8(d) the three modes are nearly in-phase; in Fig. 8(e) the LP_{01} and LP_{02} modes are

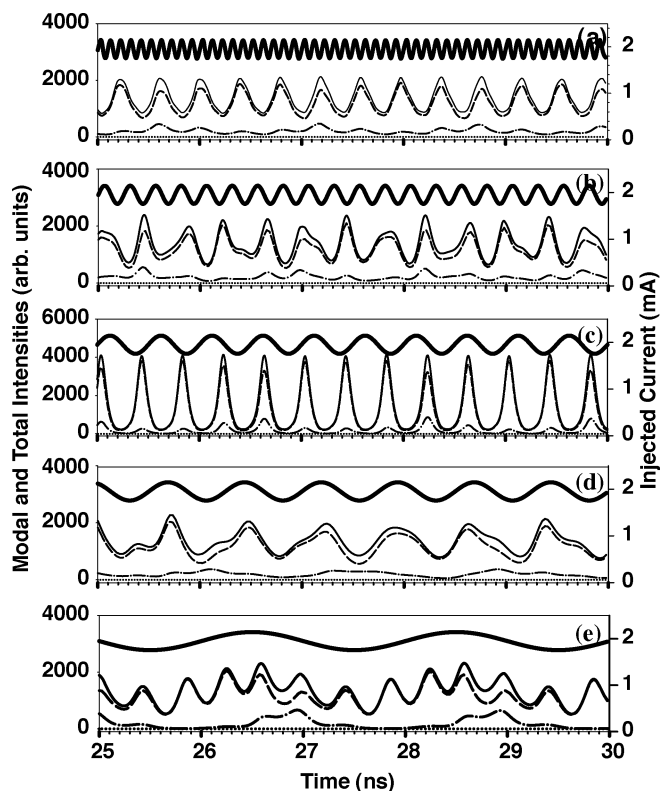


Fig. 6. Total intensity (thin solid line) and modal intensities (LP₀₁: dashed line; LP₀₂: dot-dashed line) as a function of time for different modulation periods. $I_0 = 1.95$ mA and $\delta = 0.1$ ns. (a) $T_{\text{mod}} = 0.1$ ns. (b) $T_{\text{mod}} = 0.25$ ns. (c) $T_{\text{mod}} = 0.4$ ns. (d) $T_{\text{mod}} = 0.75$ ns. (e) $T_{\text{mod}} = 2$ ns. The thick line shows the injection current.

in anti-phase while the LP₀₃ oscillates in-phase with the sum of the LP₀₁ and LP₀₂ modal intensities.

In multimode operation, there is a resonant behavior which is similar to that found in the single-mode case. This resonance is revealed by plotting the average, maximum, and minimum value of the total intensity as a function of the modulation period [shown in Fig. 9 for the two injection currents considered, $I_0 = 1.95$ mA and $I_0 = 3.2$ mA]. For low amplitude modulation [Fig. 9(a) and (b)], there is a symmetric peak: the maximum value of I_{max} and the minimum value of I_{min} both occur for $T \sim T_{\text{RO}}$; for larger amplitude modulation [Fig. 9(c) and (d)], there is a distortion of the resonance that suggests that for even larger δ bistability might occur.

Finally, let us assess the generality of the above results by considering different delay times and modal frequencies. Fig. 10 displays results for fixed T_{mod} ($T_{\text{mod}} \sim T_{\text{RO}}$) and different τ . We show results corresponding to a large injection current (such that the laser supports three transverse modes), but qualitatively the same effect of the delay time was observed when the laser operates in single mode or in two transverse modes. Under the resonant modulation condition $T_{\text{mod}} \sim T_{\text{RO}}$, the laser output exhibits pulses of period T_{mod} for all τ , which are in anti-phase with the injection current. It is observed that for small τ the pulses are regular and the transverse modes are in-phase [Fig. 10(a)], while for large τ the pulses are irregular and a more complex transverse-mode dynamics occurs, with fast in-phase pulses of the three modes combined with a longer-time scale anti-phase behavior of the LP₀₁ and LP₀₂

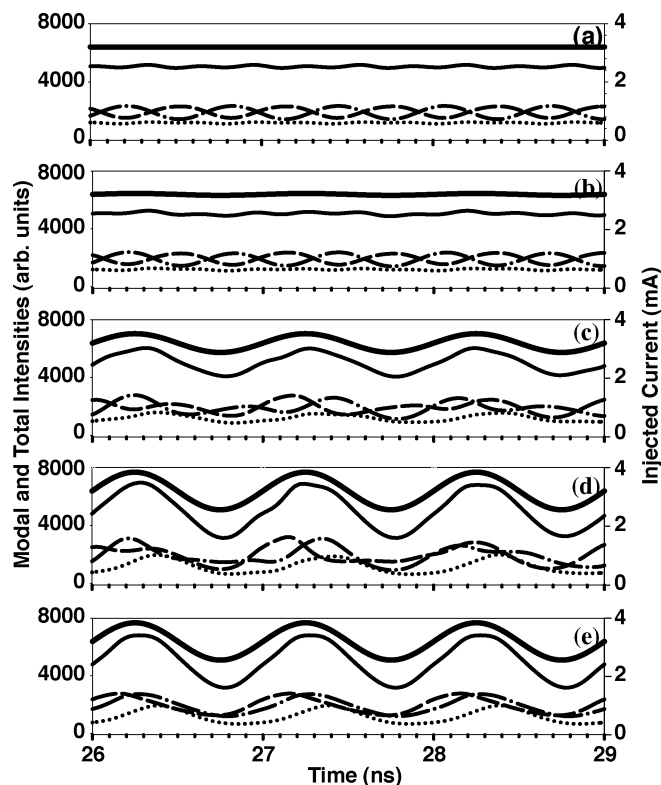


Fig. 7. Total output intensity (thin solid line) and modal intensities (LP₀₁: dashed line; LP₀₂: dot-dashed line; LP₀₃: dotted line) as a function of time for different modulation amplitudes. $I_0 = 3.2$ mA and $T_{\text{mod}} = 1$ ns. (a) $\delta = 0$. (b) $\delta = 0.01$. (c) $\delta = 0.1$. (d) $\delta = 0.2$. (e) $\delta = 0.2$ and no feedback ($k = 0$). The thick line shows the injection current.

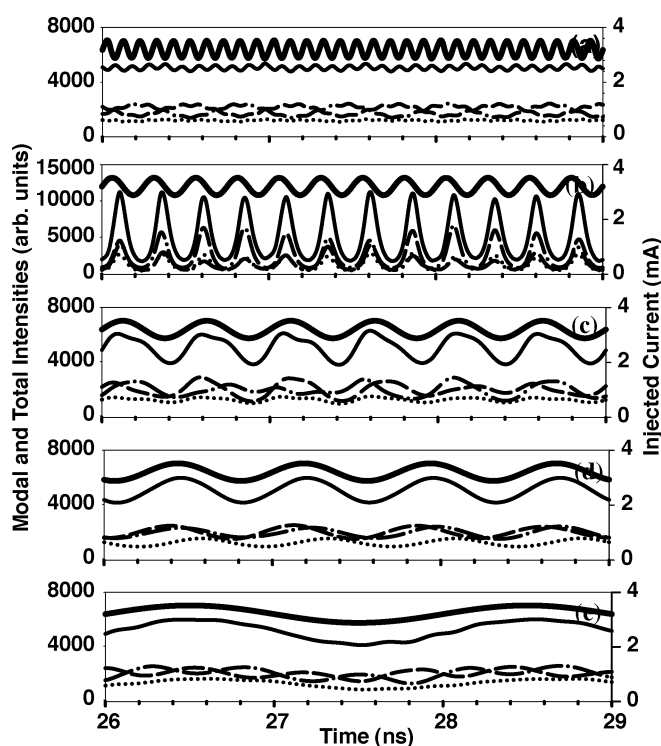


Fig. 8. Total output intensity (thin solid line) and modal intensities (LP₀₁: dashed line; LP₀₂: dot-dashed line; LP₀₃: dotted line) as a function of time for different modulation periods. $I_0 = 3.2$ mA and $\delta = 0.1$. (a) $T_{\text{mod}} = 0.1$ ns. (b) $T_{\text{mod}} = 0.25$ ns. (c) $T_{\text{mod}} = 0.5$ ns. (d) $T_{\text{mod}} = 0.75$ ns. (e) $T_{\text{mod}} = 2$ ns. The thick line shows the injection current.

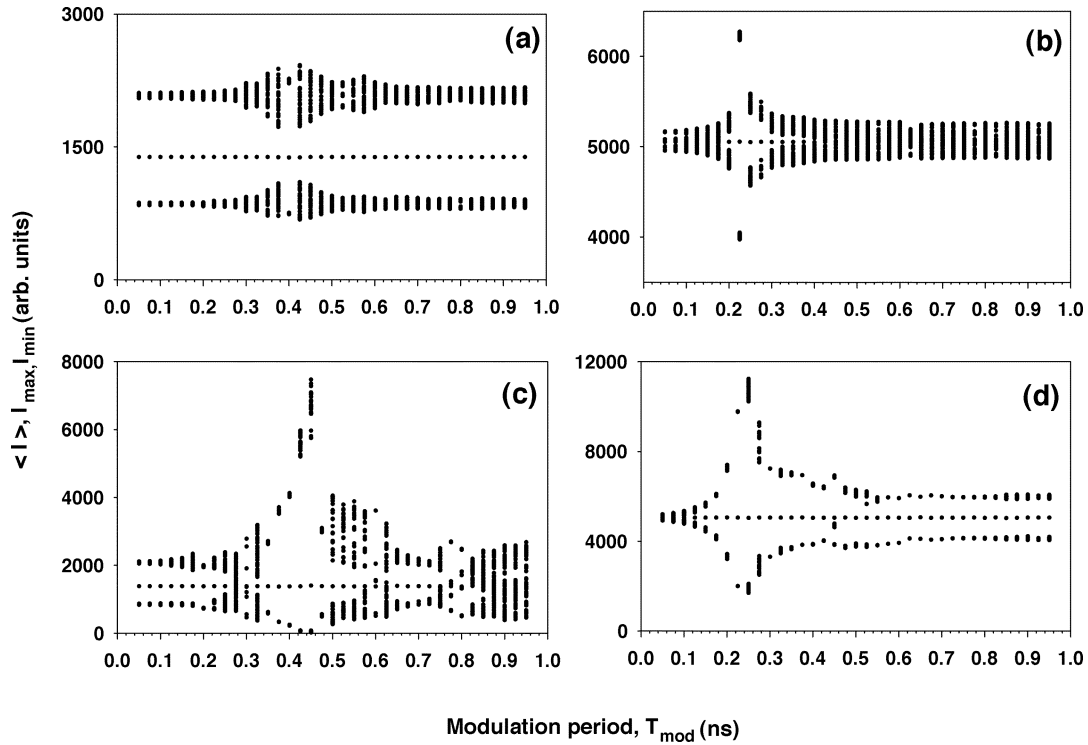


Fig. 9. Maximum, minimum, and average values of the total intensity oscillations as a function of the modulation period. (a) $I_0 = 1.95$ mA, $\delta = 0.01$. (b) $I_0 = 3.2$ mA, $\delta = 0.01$. (c) $I_0 = 1.95$ mA, $\delta = 0.1$. (d) $I_0 = 3.2$ mA, $\delta = 0.1$.

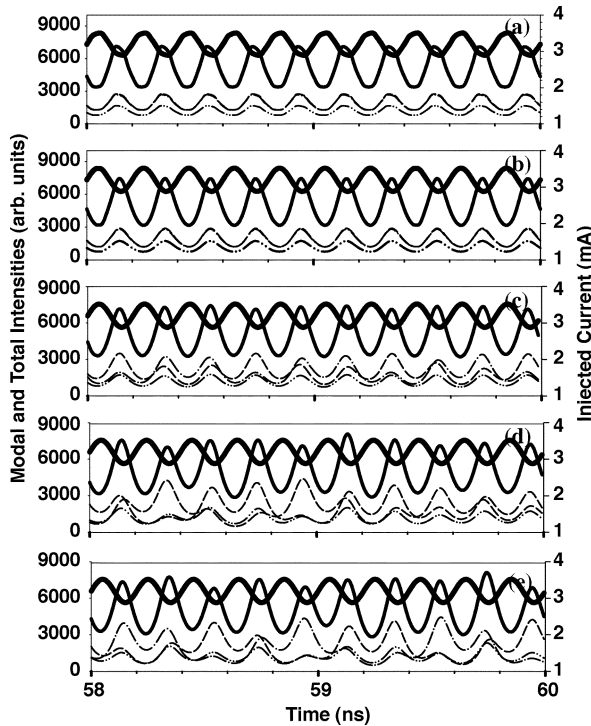


Fig. 10. Total output intensity (thin solid line) and modal intensities (LP₀₁: dashed line; LP₀₂: dot-dashed line; LP₀₃: dotted line) as a function of time for different delay times. $I_0 = 3.2$ mA, $\delta = 0.1$, $T_{\text{mod}} = 0.2$ ns. (a) $\tau = 0.1$ ns. (b) $\tau = 0.7$ ns. (c) $\tau = 1$ ns; (d) $\tau = 3$ ns. (e) $\tau = 5$ ns. The thick line shows the injection current.

modes [Fig. 10(e)]. Fig. 11 displays results for the same values of τ and $T_{\text{mod}} \gg T_{\text{RO}}$. It can be observed that the total output is in-phase with the injection current for all τ , the value of τ affecting the underlying transverse-mode dynamics, which is

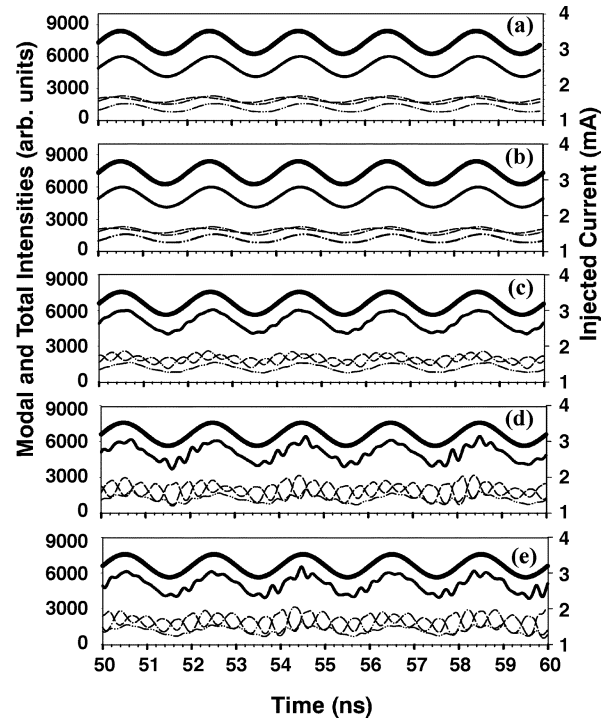


Fig. 11. The same is in Fig. 10 but $T_{\text{mod}} = 2$ ns.

nearly in-phase for short τ and more complex (with anti-phase oscillations of the LP₀₁ and LP₀₂ modes) for longer τ . For short delay times, the plot of I_{max} , I_{min} , and $\langle I \rangle$ versus T_{mod} reveals periodic behavior with a simple resonant peak [similar to that shown in Fig. 3(a)], while for long delay times the dynamics is quasi-periodic and the resonant peak is more complex [as that shown in Fig. 9(b)].

In the simulations presented so far, we have assumed that the feedback field is in-phase with the cavity field, i.e., that the feedback phases are $\omega_i\tau = 2n\pi$. In single-mode operation, the selection of a particular value of the feedback phase does not influence the laser dynamics (it leads to a global shift of the frequencies of the external cavity modes, as was shown, e.g., in [24]–[26]). In multimode operation, the feedback phases could, in principle, have a more important influence. Our simulations indicate that in general the values of $\omega_i\tau$ do not, in fact, play a significant role in the laser dynamics. Simulations performed with realistic values for the modal frequencies ω_i yield similar results to those presented in Figs. 10 and 11. However, for slow modulation and short delay times, we have observed a pulsing behavior which occurs for very particular irrational values of $\omega_i\tau$.

IV. SUMMARY AND CONCLUSION

The effect of direct modulation on the transverse-mode dynamics of VCSELS with weak optical feedback has been studied numerically. We have analyzed three different feedback-induced regimes: single-mode periodic oscillations of the fundamental LP_{01} mode, in-phase oscillations of the LP_{01} and LP_{02} modes, and anti-phase oscillations of the LP_{01} and LP_{02} modes. The modulation amplitude and period were taken as control parameters. We found that these feedback-induced transverse-mode regimes are generally robust under weak current modulation. When the modulation is slow, the feedback and modulation effects superpose such that some features of the dynamics are induced by the modulation and others are induced by the feedback. For example, in Fig. 7(c) and (d), there are anti-phase oscillations of the LP_{01} and LP_{02} modes which are due to the optical feedback, and there is a modulation of the total output which is due to the current modulation. When the period of the modulation is close to the internal relaxation oscillation period, a resonant pulsing behavior of the laser output was observed even for weak modulation. In the pulsing regime, the laser operates either in a single-transverse mode or in several transverse modes. In the latter case, the transverse modes exhibit in-phase pulses. These results might be of interest for high-bit-rate optical data transmission systems based on multimode VCSELS.

REFERENCES

- [1] "Special Issue on VCSELS and Optical Interconnects," *Proc. SPIE*, vol. 4942, 2003.
- [2] M. San Miguel, *Semiconductor Quantum Optoelectronics*, A. Miller, M. Ebrahimzadeh, and D. M. Finlayson, Eds. Bristol, U.K.: Institute of Physics, 1999, p. 339.
- [3] J. Sacher, D. Baums, P. Panknin, W. Elsasser, and E. O. Gobel, "Intensity instabilities of semiconductor lasers under current modulation, external light injection, and delayed feedback," *Phys. Rev. A*, vol. 45, pp. 1893–1905, 1992.
- [4] C. R. Mirasso and E. Hernández-García, "Effects of current modulation on timing jitter of single-mode semiconductor lasers in short external cavities," *IEEE J. Quantum Electron.*, vol. 30, pp. 2281–2286, Sept. 1994.
- [5] A. T. Ryan, G. P. Agrawal, G. R. Gray, and E. C. Gage, "Optical-feedback-induced chaos and its control in multimode semiconductor lasers," *IEEE J. Quantum Electron.*, vol. 30, pp. 668–679, Mar. 1994.
- [6] J. Dellunde, M. C. Torrent, C. R. Mirasso, and J. M. Sancho, "Turn-on-time statistics of modulated lasers subjected to resonant weak optical feedback," *Phys. Rev. A*, vol. 52, pp. 4187–4193, 1995.

- [7] Y. Takiguchi, Y. Liu, and J. Ohtsubo, "Low-frequency fluctuation induced by injection-current modulation in semiconductor lasers with optical feedback," *Opt. Lett.*, vol. 23, pp. 1369–1371, 1998.
- [8] —, "Low-frequency fluctuation and frequency-locking in semiconductor lasers with long external cavity feedback," *Opt. Rev.*, vol. 6, pp. 399–401, 1999.
- [9] D. W. Sukow and D. J. Gauthier, "Entraining power-dropout events in an external-cavity semiconductor laser using weak modulation of the injection current," *IEEE J. Quantum Electron.*, vol. 26, pp. 175–183, Feb. 2000.
- [10] J. M. Mendez, R. Laje, M. Giudici, J. Aliaga, and G. B. Mindlin, "Dynamics of periodically forced semiconductor laser with optical feedback," *Phys. Rev. E*, vol. 63, p. 066218, 2001.
- [11] F. Marino, M. Giudici, S. Barland, and S. Balle, "Experimental evidence of stochastic resonance in an excitable optical system," *Phys. Rev. Lett.*, vol. 88, p. 040601, 2002.
- [12] M. Sciamanna, C. Masoller, N. B. Abraham, F. Rogister, P. Mégret, and M. Blondel, "Different regimes of low-frequency fluctuations in vertical-cavity surface-emitting lasers," *J. Opt. Soc. Amer. B*, vol. 20, pp. 37–44, 2003.
- [13] M. Sondermann, H. Bohnet, and T. Ackemann, "Low-frequency fluctuations and polarization dynamics in vertical-cavity surface-emitting lasers with isotropic feedback," *Phys. Rev. A*, vol. 67, p. 021 802, 2003.
- [14] N. Fujiwara, Y. Takiguchi, and J. Ohtsubo, "Observation of low-frequency fluctuations in vertical-cavity surface-emitting lasers," *Opt. Lett.*, vol. 28, pp. 896–898, 2003.
- [15] A. V. Naumenko, N. A. Loiko, M. Sondermann, and T. Ackemann, "Description and analysis of low-frequency fluctuations in vertical-cavity surface-emitting lasers with isotropic optical feedback by a distant reflector," *Phys. Rev. A*, vol. 68, p. 033 805, 2003.
- [16] A. Valle, L. Pesquera, S. I. Turovets, and J. M. Lopez, "Nonlinear dynamics of current-modulated vertical-cavity surface-emitting lasers," *Opt. Commun.*, vol. 208, pp. 173–182, 2002.
- [17] M. Sciamanna, A. Valle, P. Mégret, M. Blondel, and K. Panajotov, "Nonlinear polarization dynamics in directly modulated vertical-cavity surface-emitting lasers," *Phys. Rev. E*, vol. 68, p. 016 207, 2003.
- [18] M. S. Torre, C. Masoller, and P. Mandel, "Transverse mode dynamics in vertical-cavity surface-emitting lasers with optical feedback," *Phys. Rev. A*, vol. 66, p. 053817, 2002.
- [19] A. Valle, J. Sarma, and K. A. Shore, "Dynamics of transverse-mode competition in vertical-cavity surface-emitting laser-diodes," *Opt. Commun.*, vol. 115, pp. 297–302, 1995.
- [20] —, "Spatial holeburning effects on the dynamics of vertical-cavity surface-emitting laser-diodes," *IEEE J. Quantum Electron.*, vol. 31, pp. 1423–1431, 1995.
- [21] R. Lang and K. Kobayashi, "External optical feedback effects on semiconductor injection laser properties," *IEEE J. Quantum Electron.*, vol. QE-16, pp. 347–355, Mar. 1980.
- [22] M. S. Torre, C. Masoller, P. Mandel, and K. A. Shore, "Enhanced sensitivity to current modulation near dynamic instability in semiconductor lasers with optical feedback and optical injection," *J. Opt. Soc. Amer. B*, vol. 21, no. 2, pp. 302–306, 2004, to be published.
- [23] M. S. Sodha and A. K. Ghatak, *Inhomogeneous Optical Waveguides*. New York: Plenum, 1977.
- [24] T. Erneux, G. H. M. van Tartwijk, D. Lenstra, and A. M. Levine, "Determining Lang and Kobayashi Hopf bifurcation points," *Proc. SPIE*, vol. 2399, pp. 170–181, 1995.
- [25] G. H. M. van Tartwijk and D. Lenstra, "Semiconductor-lasers with optical-injection and feedback," *Quantum Semiclass. Opt.*, vol. 7, pp. 87–143, 1995.
- [26] J. Javaloyes, P. Mandel, and D. Pieroux, "Dynamical properties of lasers coupled face to face," *Phys. Rev. E*, vol. 67, p. 036201, 2003.

Maria S. Torre received the Licenciada en Física (M.Sc.) and the Ph.D. degrees from the Universidad Nacional del Centro de la Provincia de Buenos Aires (UNCPBA), Buenos Aires, Argentina. Her research was primarily in external driven laser physics.

From 1995 to 1997, she was a Postdoctoral Fellow with the Photonics Technology Department, ETSI Telecomunicaciones, Universidad Politécnica de Madrid, Madrid, Spain. Her research was in quantum-well semiconductor laser modeling. Since 1988, she has been a member of the Quantum Electronic Group, Physics Institute "Arroyo Seco," UNCPBA. She is currently a Research Professor at the Facultad de Ciencias Exactas, UNCPBA. Her research topics include modeling and dynamics of vertical-cavity surface-emitting lasers, dynamics of semiconductor laser with external optical feedback, and diffusion effects in semiconductor lasers.

Cristina Masoller was born in Montevideo, Uruguay, in 1963. She received the M.Sc. degree in physics from the Universidad de La Republica, Montevideo, Uruguay, in 1991 and the Ph.D. degree in physics from Bryn Mawr College, Bryn Mawr, PA, in 1999.

She was a Visiting Professor with the Physics Department, Universitat de les Illes Balears, Spain (September–October 2001 to February–March 2002 and September 2002) and a Visiting Researcher with the School of Informatics, University of Wales, Bangor, U.K. (October 2002–January 2003 and October–November 2003). Since 1993, she has been with the Physics Department, School of Sciences, Universidad de la Republica, where she is an Associate Professor. In 2003, she became a Regular Associate of the Abdus Salam International Centre for Theoretical Physics, Trieste, Italy. She has authored or coauthored over 40 journal papers. Her research interests include theoretical modeling of chaotic systems, synchronization and stochastic phenomena, nonlinear dynamics of semiconductor lasers, and timedelayed systems.

Paul Mandel (M'89) was born in Geneva, Switzerland, in 1942. He received the M.D., Ph.D., and the Thèse d'agrégation degrees all from the Université Libre de Bruxelles, Brussels, Belgium, in 1965, 1969, and 1980, respectively.

He is with the National Fund for Scientific Research (Belgium) and also with the Theoretical Nonlinear Optics Group, Université Libre de Bruxelles, where he is currently teaching nonlinear optics and quantum optics in the Science and Applied Science faculties. Since 1972, his research topics have been in the field of quantum and semiclassical optics, with contributions to the theory of stability in lasers (gas, solid state, and semiconductor lasers), optical bistability and $\chi^{(2)}$ nonlinear media, including time-dependent control parameters, multimode dynamics and transverse effects.

Dr. Mandel is a Fellow of the Optical Society of America.

K. Alan Shore (M'88–SM'95) graduated in mathematics from the University of Oxford, Oxford, U.K., and received the Ph.D. degree from University College, Cardiff, Wales, U.K. His thesis work was concerned with the electrical and optical properties of double-heterostructure semiconductor lasers.

He was a Lecturer with the University of Liverpool, Liverpool, U.K. (1979–1983) and then at the University of Bath, Bath, U.K., where he became Senior Lecturer (1986), Reader (1990), and Professor (1995). In 1995 he was appointed to the Chair of Electronic Engineering, University of Wales, Bangor, Wales, U.K., where he is currently the Head of the School of Informatics. He is the Director of "Industrial and Commercial Optoelectronics" (ICON), a Welsh Development Agency Centre of Excellence, which has a mission to "make light work" through the utilization of Bangor optoelectronics expertise and facilities. He is also the Deputy Chair of the Welsh Optoelectronics Forum. His research work has been principally in the area of semiconductor optoelectronic device design and experimental characterization with particular emphasis on nonlinearities in laser diodes and semiconductor optical waveguides. He has authored or coauthored over 650 contributions to archival journals, books and technical conferences. He was a Visiting Researcher with the Center for High Technology Materials, University of New Mexico, Albuquerque, in 1987. He received a Royal Society Travel Grant to visit universities and laboratories in Japan in July 1988. In 1989, he was a Visiting Researcher with the Huygens Laboratory, Leiden University, The Netherlands. During the summers of 1990 and 1991, he worked at the Teledanmark Research Laboratory and the MIDIT Center of the Technical University of Denmark, Lyngby. He was a Guest Researcher with the Electrotechnical Laboratory (ETL) Tsukuba, Japan, in 1991. In 1992, he was a Visiting Professor with the Department of Physics, University de les Illes Balears, Palma-Mallorca, Spain. He was a Visiting Lecturer with the Instituto de Fisica de Cantabria, Santander, Spain in June 1996 and 1998 and a Visiting Researcher with the Centre for Laser Applications, Department of Physics, Macquarie University, Sydney, Australia, in July/August 1996, 1998, 2000 and April 2002. In July/August 2001 he was a Visiting Researcher with the ATR Adaptive Communications Laboratories, Kyoto, Japan. His current research interests include multiwave mixing and optical switching in semiconductor lasers, design and fabrication of intersubband semiconductor lasers and organic semiconductor lasers, dynamics of vertical-cavity semiconductor lasers, and applications of nonlinear dynamics in semiconductor lasers to optical data encryption.

Dr. Shore cofounded and acts as Organizer and Programme Committee Chair for the international conference on Semiconductor and Integrated Optoelectronics (SLOE) which, since 1987, has been held annually in Cardiff, Wales, UK. He was Programme Chair for the UK National Quantum Electronic Conference (QE'13) and was European Liaison Committee chair for the OSA Integrated Photonics Research (IPR'98) conference in Victoria, BC, Canada, 1998. He was a member of the programme committee for IPR'99 Santa Barbara, CA, July 1999 and also the European Conference on Integrated Optics (ECIO) Torino, Italy, in April 1999. He was a co-organizer of a Rank Prize Symposium on Nonlinear Dynamics in Lasers held in the Lake District, UK in August 2002. He was a technical committee member for CLEO(Europe) 2003.